Sensor-Based Formation Control of Autonomous Marine Robots

Guilherme Sanches
guilherme.sanches@ist.utl.pt

Instituto Superior Técnico, Lisboa, Portugal

October 2015

Abstract

In the context of underwater ocean exploration, challenging underwater mission emerge. In these scenarios the presence of people is not desirable on the account of the harsh conditions of the deep sea or due to the long diving periods required to undertake the missions. On the other hand, tricky technological challenges arise, as the lack of GPS signal or Wi-Fi communications. Motivated by these scenarios, this paper aims to design a strategy capable of executing cooperative underwater missions using a group of asymmetric robots. To this end, the issue of ocean currents is tackle, with a new method to cancel the currents effect on path-following being presented. An intense study of the consequences of adapting straight line guidance laws to curved paths is put forward showing interesting results. Next, in order to make the vehicles follow the path in a formation, it is shown a coordination strategy capable of coordinating the vehicles. Although, because communication are made in discrete fashion and due to communication made through acoustic modems, that are affected by intermittent failures and long transmission periods, estimator are designed to estimate the underwater vehicles position and the formation state of the flock of robots.

Keywords: Cooperative path-following, Curved paths following, Ocean currents estimation and compensation, Underwater position estimation

1. Introduction

Recent technological developments have aroused a widespread interest on motion control of multiple vehicles. Indeed, as the hardware is progressively cheaper and smaller, the possibility of building and operating several small autonomous marine vehicles (AUV) arises. A group of these vehicle can be used in a manifold of applications, like ocean floor mapping, underwater structure inspection, among others. For these reasons, a number of formation control algorithms can be seen in the literature in the scope of multiple vehicles motion control [1], [16] and [4]. For reasons of conciseness, in this paper we will address a particular scenario where two underwater vehicles (UV) preform a task, such as ocean floor mapping, trough a pre-defined path and a surface vehicle (SV), equipped with an ultra short baseline (USBL) and global positioning system (GPS), sends the UVs messages with their inertial positions, through acoustic modems. Nevertheless, to be able to control a group of vehicles it is first necessary to control a single vehicle. To this end, two main strategies have been in focus, trajectory-tracking (TT) and path-following (PF). The first requires a vehicle to follow a path parameterized in space and time, whereas the latter only requires the vehicle to follow a path parameterized in space. It has been reported in the literature that smoother control signals are generated by PF [15], [6].

In this work we will address PF motion control problem for underactuated vehicles, using inner-outer loops decoupling. The inner loop controller is a heading autopilot, with control in yaw, and the outer loop consists of a guidance law. These two elements solve the PF problem. For the purpose of this paper it is considered that an inner loop is already installed on the vehicles, so it will not be designed here. The guidance laws can be taken from the literature to follow straight line path [8], [9].

However, it is commonly necessary to follow paths that consist of arcs and straight lines. Nevertheless, an adaption can be made to use straight line guidance laws in curved paths [3]. Even so, there is a lack of analysis on the consequences of this adaption in the literature. Since it is not clear that this scheme is able to bring the distance of the vehicle to the path, also known as cross-track error, to zero. A study on this matter is held here.

Another issue that affects a vehicle's motion control, in open ocean environments, is ocean current. When a vehicle is affected by ocean currents a simple guidance law is not able to drive the cross-track error to zero. A number of solutions to this problem have been reported [8], [14]. In the first reference it is suggested to use an integral term of the cross-track error in the guidance law. Nonetheless, this solution presents a poor behavior when the heading, of the path to be followed, changes frequently. In the latter a current observer is used to estimate the current in the inertial reference frame. This estimate is then fed to the guidance law, that, in turn, cancels the current. We will present yet another strategy to solve this problem that does not depend on the guidance law.

In order to obtain coordination among several vehicles a coordination scheme has to be devised. We can resort to algebraic graph theory and design a scheme such as the one presented in [16].

Finally, it as to be taken into account that underwater communication are made through acoustic modem and have low bandwidth and data rate. Furthermore, the communications made have a high probability of failing. It is, thus, necessary to design a position estimator and a coordination state estimator. The first allows for the underwater vehicles to be able to estimate their path between communications and the second will allow for a vehicle to estimate the coordination states of the rest of the flock while no coordination state related communication occurs.

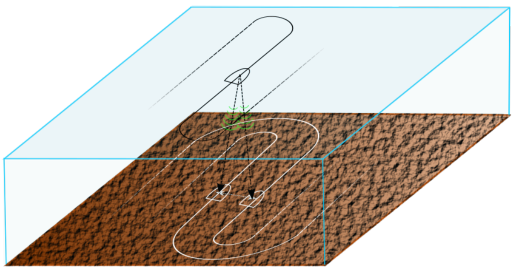

Figure 1: Cooperative path following concept. The bottom vehicles need to preform some operation underwater and the top vehicle helps with inertial localization.

2. Guidance Laws for Curved Paths

As it was said before, there is extensive literature on the subject of guidance laws for planar motion. Most of which were designed to follow straight line paths [8], [9]. However, one of the most executed maneuvers, the lawnmower, consists of a succession of straight lines and arcs. For the vehicles to be able to follow curved paths, such as the arc segments, this laws can be adapted [3]. Nevertheless, there is no study about the consequences of this adaptation in what concerns the cross-track error, that is, it is not proven that this scheme can bring the cross-track error to zero. That is what we aim to do in this section.

2.1. Path-Following of Constant Curvature Paths

As we want to study what the guidance law alone can provide to reduce the cross-track error, the dynamics of the vehicle will not be considered. Hence, consider the kinematic model

$$\dot{\boldsymbol{p}} = R(\psi)\boldsymbol{v} + \boldsymbol{V}_c \tag{1}$$

where $\dot{p} = [\dot{x}, \dot{y}]^T$ is the inertial position derivative, $R(\psi)$ is the rotation matrix and $\boldsymbol{v} = [u, v]^T$, that is, a vector with the surge and sway speeds. Furthermore, $\boldsymbol{V}_c$ is the current's speed measured in the inertial frame. For the study in this section the dynamics are not considered, so the heading converges instantly to the desired value, secondly the sway speed is considered to be $v \approx 0$ and finally the currents speed is assumed to be zero as well, $\boldsymbol{V}_c = 0$. Therefor, the kinematic model 1 can be simplified to

$$\begin{bmatrix} \dot{x} \\ \dot{y} \end{bmatrix} = u \begin{bmatrix} \cos(\psi) \\ \sin(\psi) \end{bmatrix} \tag{2}$$

Consider the guidance laws

$$\psi_d^{LOS} = \arctan\left(-\frac{e}{d}\right) + \chi_p \tag{3}$$

$$\psi_d^{P.Maurya} = \arcsin\left(sat\left(-\frac{k_1}{u}e\right)\right) + \chi_p \tag{4}$$

where e is the cross-track error, u is the surge speed, d is the lookahead distance and χ_p is the path angle, k_1 a gain and the term $sat(\cdot) \in [-1, 1]$ is a saturation function.

It is assumed, for now, that the paths have constant curvature, that is, they are circles or arcs. This restriction on the type of path will be lifted further on this work. The line tangent to the curve in the orthogonal projection of the vehicle's position in the curve, can be seen as an instantaneous straight line, and can be used to generate heading references. This point corresponds to point 1 in figure 2. To study this issue we will use the so-called *Serret-Frenet* equation, inspired by its applications in [13], [7] and [10].

There are three variables to describe the Serret-Fernet(SF) parameterization. Their expressions, for a generic path, are as follows

$$\dot{s} = \frac{u\cos(\psi - \chi_p)}{1 - c(s)e} \tag{5}$$

is the curvilinear distance traveled in the path,

$$\dot{e} = u\sin(\psi - \chi_p) \tag{6}$$

is the vehicle's position component orthogonal to the path, measured in the SF frame, which ultimately is the cross-track error, and

$$\dot{\chi}_p = c(s)\dot{s} \tag{7}$$

where χ_p is the angle of the tangent line of the curve, making $\dot{\chi}_p$ the course rate, ψ is the heading of the vehicle and $c(s)$ the curvature at point s. As the curvature of a circle with radius R is the inverse of the radius

$$c(s) = \frac{1}{R} \tag{8}$$

For now, it is considered that the SF frame's position is always the orthogonal projection of the vehicle's position in the curve. Thus, the dynamics of e is expressed by equation 6. The heading angles ψ will be given by the guidance laws above described in 3 and 4.

Making use of nonlinear control systems theory, we select equation 9 as the Lyapunov's candidate function, as it can be seen that $V > 0 \; \forall \; e \in \mathbb{R}\backslash\{0\}$ and $V = 0$ for $e = 0$.

$$V(e) = \frac{1}{2}e^2 \tag{9}$$

Substituting in equation 6 equation 3 we obtain

$$\begin{aligned} \dot{e} &= u \sin(\psi - \chi_p) \\ &= u \sin\left(\arctan\left(-\frac{e}{d}\right)\right) \\ &= -u\frac{e}{\sqrt{d^2+e^2}} \end{aligned} \tag{10}$$

differentiating the candidate function 9 and substituting by 10 we obtain

$$\begin{aligned} \dot{V} &= e\dot{e} \\ &= -u\frac{e^2}{\sqrt{d^2+e^2}} < 0, \forall e \neq 0 \end{aligned} \tag{11}$$

Hence, as the surge speed is assumed to be always positive, $e = 0$ is a globally asymptotically stable equilibrium point of the error function. Therefor, it is proven that the error converges to zero in what concerns the kinematics of the vehicle.

The same methodology can be applied to the P. Maurya guidance law. Substituting in equation 6 equation 4, and considering that the argument of the $sat(\cdot)$ function is not saturated, we obtain

$$\begin{aligned} \dot{e} &= u \sin\left[\arcsin\left(sat\left(-\frac{k_1}{u}e\right)\right)\right] \\ &= -k_1 e \end{aligned} \tag{12}$$

Which, unlike the line of sigh's case, can be simply solved to give the final result

$$e(t) = e_0 \exp^{-k_1 t} \tag{13}$$

where e_0 is the initial error. In the case of the guidance law suggested by P. Maurya we can verify that the guidance law drives the error globally exponentially to zero.

2.2. Guidance for Path Following along Curved Trajectories

2.2.1 Guidance Law Deduction

It is also worth noting other strategies in the literature, like [11]. In this case instead of the lookahead distance being a target in a line tangent to the curve, it is, in fact, part of the curve, that is the d is measured along path.

Starting by defining the problem:

Problem 1 (Along Path Line of Sight)**.** *Consider the figure 2. Given a circular path with radius R, centered at the origin of the referential and a vehicle in position (x, y), that is not affected by side slip, design a guidance law for ψ_d that aims for a point in the curve that is a distance d ahead of the projection of the vehicle in the curve (x_1, y_1), that is, point (x_2, y_2). Furthermore $(x_i, y_i), i = 1, 2$, are the Cartesian coordinates of points 1 and 2, respectively.*

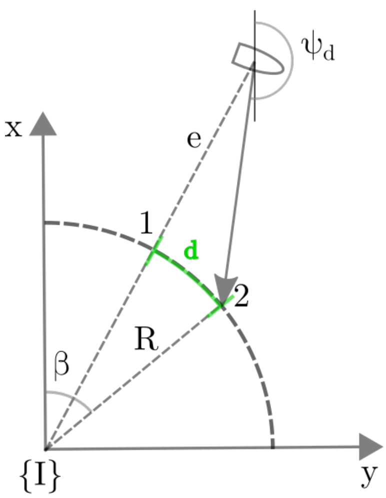

Figure 2: Symbol definitions and vehicle and path geometry.

We can express the desired heading as

$$\psi_d = atan2(y_2 - y, x_2 - x) \tag{14}$$

where y_2 and x_2 are equal to

$$\begin{aligned} x_2 &= R\cos(\beta) \\ y_2 &= R\sin(\beta) \end{aligned} \tag{15}$$

because the circle is centered at the origin of the referential β can be written as

$$\beta = \frac{d}{R} + atan2(y,x) \tag{16}$$

Now we can substitute equation 16 into 15 and then into 14, to obtain

$$\begin{aligned}\psi_d =& atan2\left(R\sin(\beta) - y, R\cos(\beta) - x\right)\\ =& atan2\left(R\sin\left(\frac{d}{R} + atan2(y,x)\right) - y,\right.\\ &\left.R\cos\left(\frac{d}{R} + atan2(y,x)\right) - x\right)\end{aligned} \tag{17}$$

after some algebra, we can simplify equation 17 to

$$\begin{aligned}\psi_d = atan2&\left(\frac{Ry\cos\left(\frac{d}{R}\right) + Rx\sin\left(\frac{d}{R}\right)}{\sqrt{x^2+y^2}} - y,\right.\\ &\left.\frac{Rx\cos\left(\frac{d}{R}\right) - Ry\sin\left(\frac{d}{R}\right)}{\sqrt{x^2+y^2}} - x\right)\end{aligned} \tag{18}$$

Now we have a complete expression of the guidance law, that gives us the reference heading angle for each position in the plane.

2.2.2 Guidance Law Stability Analysis

Let us now analyze the effect of the guidance law 18 on the cross-track error.

Firstly, we express the error as

$$e = \sqrt{x^2+y^2} - R \tag{19}$$

This function can the differentiated to obtain 20. Then substituting $\dot{x}$ and $\dot{y}$ using equation 2, we get

$$\begin{aligned}\dot{e} &= \frac{x\dot{x} + y\dot{y}}{\sqrt{x^2+y^2}}\\ &= u\frac{x\cos(\psi) + y\sin(\psi)}{\sqrt{x^2+y^2}}\end{aligned} \tag{20}$$

substituting equation 18 in 20, after some algebra, we get

$$\dot{e} = -\frac{\left(u\sqrt{x^2+y^2} - R\cos\left(\frac{d}{R}\right)\right)}{\sqrt{R^2 + (x^2+y^2) - 2R\left(\sqrt{x^2+y^2}\right)\cos\left(\frac{d}{R}\right)}} \tag{21}$$

For simplicity, we make the following change of variable $\xi = 1 - \cos\left(\frac{d}{R}\right)$ and from 19 we express $\sqrt{x^2+y^2} = e + R$, to obtain

$$\dot{e} = -\frac{u(e + R\xi)}{\sqrt{R^2 + (e+R)^2 - 2R(e+R)\cos\left(\frac{d}{R}\right)}} \tag{22}$$

It can be clearly seen that the point $e = -R\xi$ is an equilibrium point of the cross-track error. The same result is reported in [11].

We will now resort to Lyapunov's second method to prof its stability. Starting by defining $e^\star = -R\xi$ and $e'(t) = e(t) - e^\star$, the candidate function is the same as in 9, but this time as a function of e'. So we have

$$\begin{aligned}\dot{V}(e') &= \dot{e}'\\ &= \dot{e}e'\\ &= -\frac{u(e+R\xi)e'}{\sqrt{(e+R)^2 + R^2 - 2R(e+R)\cos\left(\frac{d}{R}\right)}}\end{aligned} \tag{23}$$

$$= -\frac{ue'^2}{\sqrt{(e' + e^\star + R)^2 + R^2 - 2R(e' + e^\star + R)\cos\left(\frac{d}{R}\right)}}$$

Hence, $e^\star$ is a globally asymptotically stable equilibrium point of the cross-track error.

The guidance law, with the lookahead distance along the path, presents a static error in the steady state, unlike the guidance laws for straight lines adapted for curved paths, which can bring the cross-track error to zero. The first two solutions to follow curved paths present themselves as better alternatives. One can intuitively understand that, for a path with constant curvature, the desired heading is always tangent to the orthogonal projection of the vehicle's position, so the tangent line should be the instantaneous desired path. This is now proven to be a solution that brings the cross-track error to zero.

2.3. Arbitrary Path

In this section we will lift the assumption of constant curvature paths, and prove that the guidance laws, of equations 3 and 4, can control the cross-track error to zero, for paths with position varying curvature.

To prove the equilibrium points for an arbitrary path following one extra degree of freedom must be added. Instead of using the orthogonal projection of the vehicle's position, a point with its own dynamics is used. This reference is the so called rabbit, as referred in [14].

The expression of the Lyapunov's candidate function is

$$V = \frac{1}{2}\left(s_1^2 + e^2\right) \tag{24}$$

The error dynamics in equation 6 and the rate of progression in 5 are modified to account for the new degree of freedom

$$\dot{s}_1 = -\dot{s}\left(1 - c(s)e\right) + u\cos(\psi - \chi_p) \tag{25}$$

$$\dot{e} = -c(s)\dot{s}s_1 + u\sin(\psi - \chi_p) \tag{26}$$

and the control law for the s is taken from [14], that is

$$\dot{s} = u\cos(\psi - \chi) + k_2 s_1 \tag{27}$$

We start by differentiating equation 24 and use equation 25 and 26 to obtain

$$\begin{aligned}\dot{V} =& \dot{s}_1 s_1 + \dot{e}e \\ =& s_1\left(-\dot{s}\left(1 - c(s)e\right) + u\cos\left(\psi - \chi_p\right)\right) + \\ & e\left(-c(s)\dot{s}s_1 + u\sin\left(\psi - \chi_p\right)\right) \\ =& - s_1\dot{s} + us_1\cos\left(\psi - \chi_p\right) + ue\sin\left(\psi - \chi_p\right)\end{aligned} \tag{28}$$

now we substitute equation 27 in 28 to obtain

$$\dot{V} = -k_2 s_1^2 + ue\sin(\psi - \chi) \tag{29}$$

only the guidance law is thus left to be substituted. It is easy to see that the the first term of equation 29 is negative definite for $s_1 \in \mathbb{R}\setminus\{0\}$. Moreover the second part is equal to equation 10 first expression when substituted in to 11, in the case of the LOS guidance, and will surely give a similar result for the case of the P. Maurya guidance.

For the case of the LOS guidance we obtain

$$\begin{aligned}\dot{V} &= -k_2 s_1^2 + ue\left(-\frac{e}{\sqrt{d^2 + e^2}}\right) \\ &= -k_2 s_1^2 - \frac{ue^2}{\sqrt{d^2 + e^2}} < 0\,\forall\, s_1, e \neq 0\end{aligned} \tag{30}$$

and for the P. Mauria guidance

$$\dot{V} = -k_2 s_1^2 - k_1 e^2 < 0\,\forall\, s_1, e \neq 0 \tag{31}$$

The same result would be obtain for the guidance law of equation 18, where the second term of equation 29 would be substituted for equation 23. In summary, the three guidance laws have stable equilibrium points for the cross-track error, in the case of arbitrary paths, as proven by Lyapunov's second method. Moreover, the first two guidance laws have bring the cross-track error to zero and the guidance law with along track lookahead presents a static error, as in section 2.1.

3. Current Estimation and Course Control

According to what was mentioned before, to be able to control the vehicles in environments such as the ocean, the ocean currents must be taken into account. In this section we design a current observer and a unit to cancel effect of ocean currents in the vehicles course.

3.1. Current Observer

In order to tackle this problem we take inspiration form [12]. Indeed, we can measures the inertial position of the vessel, using the GPS, and the speed of the vehicle's body relatively to the fluid, in the body frame, using a calibration curve or a doppler velocity log (DVL). Then, by considering equation 1, a design model relating all measured quantities can be obtain

$$M_{pv} = \begin{cases}\dot{\boldsymbol{p}}_m = R(\psi)\boldsymbol{v} + \boldsymbol{V}_c + \boldsymbol{p}_d \\ \boldsymbol{V}_m = R(\psi)\boldsymbol{v} + \boldsymbol{V}_d\end{cases} \tag{32}$$

Where $\boldsymbol{p}_d$ and $\boldsymbol{V}_d$ are position and speed disturbances, respectively. With the model M_{pv} we are now able to obtain the current observer

$$F = \begin{cases}\dot{\hat{\boldsymbol{p}}} = k1\left(\boldsymbol{p}_m - \hat{\boldsymbol{p}}\right) + \boldsymbol{V}_m + \hat{\boldsymbol{V}}_c \\ \dot{\hat{\boldsymbol{V}}}_c = k_2\left(\boldsymbol{p}_m - \hat{\boldsymbol{p}}\right)\end{cases} \tag{33}$$

where $\hat{\boldsymbol{p}}$ and $\hat{\boldsymbol{V}}_c$ are the inertial positions estimate and the current speed estimate, respectively. The filter is internally stable for any choice of constant and positive k_1 and k_2.

3.2. Current Compensation

Once the inertial current vector is known we can control our heading in order to compensate for the current and follow the desired course, set by the guidance law.

The relation between the three quantities at steak, is expressed by equation 1. As the DVL is an expensive device, a calibration curve is used to know the relative velocity between the body and the fluid. For this reason, the sway speed is once approximated $v \approx 0$. We can then obtain

$$\begin{aligned}\boldsymbol{V}_T &= R(\psi)\begin{bmatrix}u\\0\end{bmatrix} + \boldsymbol{V}_c \\ \begin{bmatrix}V_{Tx}\\V_{Ty}\end{bmatrix} &= u\begin{bmatrix}\cos(\psi)\\\sin(\psi)\end{bmatrix} + \begin{bmatrix}V_{cx}\\V_{cy}\end{bmatrix}\end{aligned} \tag{34}$$

where $\boldsymbol{V}_T = \dot{\boldsymbol{p}}$. Equation 34 can be putted into a system of equations and we would try to solve for ψ and V_{Tx}. Although, this system would be a nonlinear algebraic equations system and the solution would be hard to compute, specially in real time. An easier approach can be taken by making all the computation in a reference frame anchored in the course vector $\boldsymbol{V}_T$. For this, we have to apply a coordinate's transformation, from the inertial frame to the said reference frame, to equation 34, as follows

$$R^T(\chi_d)\begin{bmatrix}V_{Tx}\\V_{Ty}\end{bmatrix} = uR^T(\chi_d)\begin{bmatrix}\cos(\psi)\\\sin(\psi)\end{bmatrix} + R^T(\chi_d)\begin{bmatrix}V_{cx}\\V_{cy}\end{bmatrix}$$
$$\begin{bmatrix}V_{Tx}\\0\end{bmatrix} = u\begin{bmatrix}\cos(\chi_d-\psi)\\\sin(\chi_d-\psi)\end{bmatrix} + \begin{bmatrix}V_c^{\parallel}\\V_c^{\perp}\end{bmatrix} \tag{35}$$

where χ_d is the desired course angle, given by the guidance law. As we are now considering the ocean currents this is not the same as the heading of the vehicle. Moreover, notice that now the current is expressed as having one component parallel to the the course vector and another perpendicular to the course frame. We can now use the second line of the last expression in equation 35 to obtain the desired heading

$$\psi_d = -\arcsin\left(-\frac{V_c^{\perp}}{u}\right) + \chi_d \tag{36}$$

With this scheme there is no need to design a guidance law that takes into account the current's observer estimate, as it was done by [14]. The current is compensated by a unit that is not the guidance law. To sum up, this strategy is independent of the guidance law.

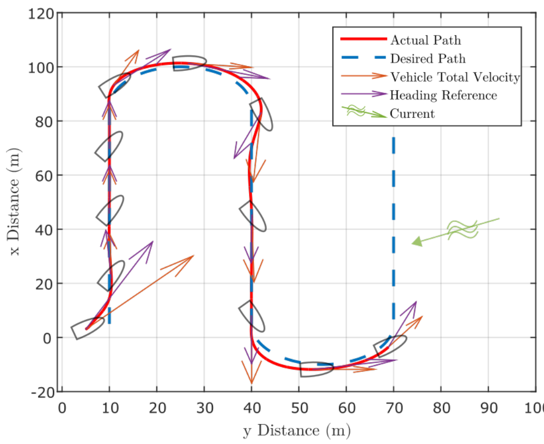

Figure 3: Position diagram of PF with currents.

3.3. Filter Robustness

For the current estimation, if we have a DVL, we know the speed of the water relative to the vehicle in each of the axis of the body frame (including in the heave direction). Nonetheless, because this is an expensive equipment, it may not be available. Thereby, as an alternative is needed, a calibration curve relates the rotations per minute (RPM) of the thrusters with the speed in the surge, u, can be used. In this section we will follow closely the work done by [14].

The equation that relates the two quantities can be obtained from the vehicle's dynamics. By considering a constant surge speed and a neglectable sway speed v we, can obtain equation 37. This obviously does not take into account the accelerations and deceleration forces, although, in after a transient period it is a good approximation and, in addition, in our case the speed reference does not change frequently or abruptly. We then expand the hydrodynamic dumping terms, to obtain

$$d_u u = \tau_u \Leftrightarrow \tau_u + X_{|u|u}|u|u + X_u u = 0 \tag{37}$$

Taking into account that $u > 0$, the equation 37 becomes a simple quadratic equation.

Although this is a useful model, it is susceptible to parametric errors, as pointed out by [14]. In the cited work a curious effect was observed: when the parametric model has errors, the current estimation is compromised, that is, wrong. Even so, the vehicle is able to drive the cross-track error to zero. This suggests that even though the estimation is wrong, there is something in the process that balances this error.

Firstly we define $e_p = \boldsymbol{p} - \hat{\boldsymbol{p}}$ and $e_v = \boldsymbol{V}_c - \hat{\boldsymbol{V}}_c$, in other words, the inertial position error and the error of the speed of the current in the inertial frame. Now we aim to study the response of the filter in the case of speed parametric error of the vehicle relatively to the water. In particular, when the error is a factor of the real value.

First, let us define the error in current estimation as

$$\hat{\boldsymbol{V}}_c = a\boldsymbol{V}_c \tag{38}$$

Making use of equations 33, 1

$$\begin{cases}\dot{e}_p = e_v + (1-a)R(\psi)\boldsymbol{v} - k_1 e_p\\ \dot{e}_v = -k_2 e_p\end{cases} \tag{39}$$

It can be seen that the equation's 39 system has as equilibrium point $e_p = 0$ and $e_v = -(1-a)R(\psi)\boldsymbol{v}$, while system 33 had an equilibrium in $e_p = 0$ and $e_v = 0$. To assess the stability of this equilibrium point we will make a variable change $e_v' = e_v - e^\star$, where $e^\star = -(1-a)R(\psi)\boldsymbol{v}$. Note that $\dot{e}_v' = \dot{e}_v$. Modifying system 39 we obtain

$$\begin{cases}\dot{e}_p = e_v' - k_1 e_p\\ \dot{e}_v' = -k_2 e_p\end{cases} \tag{40}$$

The Lyapunov candidate function use will be

$$V = \frac{1}{2}e_p^2 + \int_0^{e_v'} G(\zeta)\,\mathrm{d}\zeta \tag{41}$$

Differentiating equation 41 we get

$$\begin{aligned}\dot{V} &= \dot{e}_p e_p + G(e_v')\,\dot{e}_v'\\ &= e_p(-k_1 e_p + e_v') + G(e_v')(-k_2 e_p)\end{aligned} \tag{42}$$

where $G(e'_v)$ has to be an odd function. Let $G(e'_v) = e'_v/k_2$, if we substitute in 42 we obtain

$$\begin{aligned}\dot{V} &= e_p\left(-k_1 e_p + e'_v\right) + \left(\frac{e'_v}{k_2}\right)\left(-k_2 e_p\right) \\ &= -k_1 e_p^2\end{aligned} \tag{43}$$

Therefor, by resorting to Lyapunov's stability theory, it can be seen that the system represented by equation 40 has as globally asymptotically stable equilibrium points $e_p = 0$ and $e'_v = 0$, which implies that $e_p = 0$ and $e_v = -(1-a)R(\psi)\boldsymbol{v}$ are stable equilibrium points of equation's 39 system.

We can conclude that when the model to obtain the vehicle's speed relatively to the water is affected by parametric errors, the current observer's estimate is biased by a factor of the error. Thus, when this, wrong, estimate is fed to the guidance law, as it was done in [14], the guidance responds by giving a heading reference, in accordance with this error. Unexpectedly, the sum of this heading vector, given by the guidance, with the wrong current estimate yields the correct total velocity vector. The result obtained here show, that the error between the estimate and the real value of $\boldsymbol{V}_c$, is only in the norm. This is the mechanism that allows the behavior reported in [14].

4. Formation Control

In this section we will walk trough the steps necessary to finally attain multiple vehicle motion control.

Bearing in mind the mission scenario conceived in section 1, vehicles underwater need to know their inertial position to preform the PF task. Since underwater no GPS signal is available, a surface vehicle is needed to help the underwater vehicles learn their position. The coordination scheme adopted is described in [16] and relies on the normalized Laplacian of a graph.

Beyond the issue of coordination, there has to be taken into account stringent communications constraints. Once communications are made through acoustic networks greatly affected by intermittent failures and time-varying multipath effects, they have a great chance of failing [17]. Additionally, the speed of sound in the water is low, when compared to electromagnetic waves in the air, the data transference in acoustic networks is slow [2].

Having that said, in between communication the vehicles have not only to estimate their position but also the coordination state of the rest of the flock.

4.1. Inter Vehicle Communication and Vehicles Setup

The surface vehicle receives GPS signal, so it has access to its own inertial position. With the USBL this vehicle is also able to obtain the position of the two underwater. Having this two measurements, it is able to get inertial position of the underwater vehicles, by computing $\boldsymbol{p}_{USBL} - \boldsymbol{p}_1 = \boldsymbol{p}_j$, with j belonging to the set of underwater vehicles. The position is periodically transmitted trough the acoustic modems to the underwater vehicles, making them ware of their positions.

It is also necessary that the vehicles send to each other their coordination state, in order for them to keep an inner vehicle formation. Because the surface vehicle has the USBL measurements of vehicles 2 and 3 positions, it is able to compute the coordination state of both underwater vehicles. Nevertheless, it has to communicate its own coordination state to the underwater vehicles.

With this scheme both underwater vehicles are able to learn about their position and from there proceed with path-following.

4.2. Coordination

As it was said in section 1, a coordination scheme is necessary to achieve *cooperative path-following.* In this section, the coordination problem is formally defined and a coordination scheme to solve the aforementioned problem is shown.

The coordination problem can be formally defined, in the words of [5], as

Problem 2 (Coordination Problem)**.** *For vehicle $i = 1, \ldots, n$ derive a control law for $\dot{\gamma}_i$ as a function of local states and the variables γ_j, $j \in \mathcal{N}_i$ such that $\gamma_i - \gamma_j$, $\forall i, j$ approach a small neighborhood of zero as $t \to \infty$ and the formation travels at the speed $v_L(t)$, that is, $\dot{\gamma}_i \to v_L \; \forall \; i$.*

A simple mechanism to coordinate the vehicles is to fed the inner loops with different speed references, $\boldsymbol{u}_d$, according to its progress relatively to its counterparts. So we should include a term for the path assigned speed, that is, the speed at which the path would be traversed if all vehicles were in formation, $\boldsymbol{u}_p$, and a degree of freedom to slower the vehicle to a speed below $\boldsymbol{u}_p$, if the vehicle is upfront, or to speed up if the vehicle is behind the rest of the flock. This degree of freedom will be called $\tilde{\boldsymbol{u}}_d$. Hence we can write

$$\boldsymbol{u}_d = \boldsymbol{u}_p + \tilde{\boldsymbol{u}}_d \tag{44}$$

To adjust the speed according to the coordination state of a vehicle

$$\tilde{\boldsymbol{u}}_d = -k_\xi \tanh\left(L_D \boldsymbol{\gamma}\right) \tag{45}$$

where k_ξ is positive constant, whose value will be the absolute of upper and lower bounds of the speed correction.

This scheme based on continuous communication belongs to the outer loops and issues speed commands to the inner loops. We now move onto the final challenge, that is, to address the discrete communications among vehicles, as well as communication failures. thus, the scheme here devised will have to be reviewed in the next section.

4.3. Underwater Vehicle Self Position Estimation
In order for the underwater vehicles to estimate their position while not receiving any position measurement from the surface counterpart, we have to first consider a model of the vehicles kinematics in 1. For the same reasons above mentioned the sway speed is considered to be approximately zero. On the other hand, the surge speed is assumed to be constant and the same assumption is applied to the current's speed and to the yaw rate, having all, therefore, its derivative equal to zero. We can then build our filter model as

$$\dot{x} = \frac{\mathrm{d}}{\mathrm{d}t}\begin{bmatrix}\psi\\ \dot{\psi}\\ u\\ \boldsymbol{p}\\ \boldsymbol{V}_c\end{bmatrix} = \begin{bmatrix}\dot{\psi}\\ 0\\ 0\\ R(\psi)\begin{bmatrix}u & 0\end{bmatrix}^T + \boldsymbol{V}_c\\ 0\end{bmatrix}. \tag{46}$$

Having the model built we now have to discretize it, since it is intended to fill in the gaps between communications. To that end we fall back on the finite differences approximation, that can be represented in the following way

$$\frac{\mathrm{d}}{\mathrm{d}t}\boldsymbol{x}(t) = \frac{\boldsymbol{x}(t+\Delta t) - \boldsymbol{x}(t)}{\Delta t} = \frac{\boldsymbol{x}(k+1) - \boldsymbol{x}(k)}{\Delta t}, \tag{47}$$

where Δt is the time from one estimation to the next. To obtain the discrete time state space model we simply modify 47 to

$$\boldsymbol{x}(k+1) = \dot{\boldsymbol{x}}\Delta t + x(k) \tag{48}$$

If we apply this discrete time state space model to our continuous time state-space model in equation 46, we obtain the position estimator

$$\hat{\boldsymbol{p}}(k+1) = \left(R(\psi)\begin{bmatrix}u(k) & 0\end{bmatrix}^T + \boldsymbol{V}_c\right)\Delta t + \hat{\boldsymbol{p}}(k) \tag{49}$$

where $k \in \mathbb{N}$ is the discrete time instant when the measurements are taken. From the position estimation, we can then estimate, for the case of the straight lines, the cross-track and the coordination state errors as follows

$$\begin{bmatrix}\hat{\gamma}(k+1)\\ \hat{e}(k+1)\end{bmatrix} = R^T(\chi_p)\left(\hat{\boldsymbol{p}}(k+1) - \boldsymbol{p}_{WP}\right) \tag{50}$$

where $\boldsymbol{p}_{WP}$ is the position of the last waypoint.

For the arc segments of the lawnmoer the following estimator is used

$$\hat{\beta}(k+1) = atan2\left(\hat{y}(k+1) - y_c, \hat{x}(k+1) - x_c\right) \tag{51}$$

where (x_c, y_c) is the position of the center of the arc and in this case $\hat{\gamma} = \hat{\beta}$. As for the cross-track error in a curve, it can be given by

$$\hat{e}(k+1) = \sqrt{\left(\hat{x}(k+1) - x_c\right)^2 + \left(\hat{y}(k+1) - y_c\right)^2} \tag{52}$$

One last remark is yet to be made: whenever a position measurement message arrives from the surface vehicle, the position estimation at that instant becomes the measurement itself, that is, $\hat{\boldsymbol{p}}(t_k) = \boldsymbol{p}(k)$, where t_k is the time at the k-th discrete time instant.

4.4. Coordination State Estimation
At this point each vehicle is able to estimate its inertial position. Only the coordination state of its peers in the flock remains to be estimated. We can assume that the rate at which the $\boldsymbol{\gamma}$ parameter changes is related to the assignment speed by

$$\dot{\boldsymbol{\gamma}} = \boldsymbol{u}_d(\boldsymbol{\gamma}) \tag{53}$$

From this equality we built our continuous time state space model

$$\dot{\boldsymbol{\gamma}} = \boldsymbol{u}_p(\boldsymbol{\gamma}) - k_\xi \tanh(L_D\boldsymbol{\gamma}) \tag{54}$$

applying the finite differences derivative of equation 47, as before, we can estimate the value of $\boldsymbol{\gamma}$ in the next discrete time instant like so

$$\hat{\boldsymbol{\gamma}}(k+1) = \left(v_L(\hat{\boldsymbol{\gamma}}(k)) - k_\xi \tanh(L_D\hat{\boldsymbol{\gamma}}(k))\right)\Delta t + \hat{\boldsymbol{\gamma}}(k) \tag{55}$$

We now hold all the estimators necessary to overcome the communications constraints.

5. Simulation Results
The systems described throughout this section were implemented in matlab and simulated along with a marine vehicle dynamics and kinematics. To evaluate the performance of the position estimator, we had to force some errors in the estimates. Taking into account figure 4 it can be seen in both graphics an error in the initial position estimate. This position error forces the guidance to generate wrong heading references. However, when a new position message arrives to the vehicle's position estimator, around second 10 in the simulation, the estimator is able to produce estimations with a small error from that moment on. Ultimately, this allows the vehicle to converge to the path and follow it. Moreover, it can be observed in graphic 4(b), between $[125, 200]s$ for instance, that when the vehicles goes through a curve, some estimation error arises. This happens

because when the vehicle is in a curve the side-slip is greater, hence our model approximation of $v \approx 0$ is less accurate.

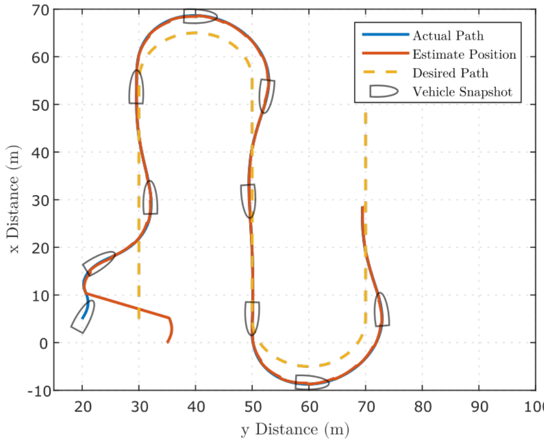

(a) Position diagram

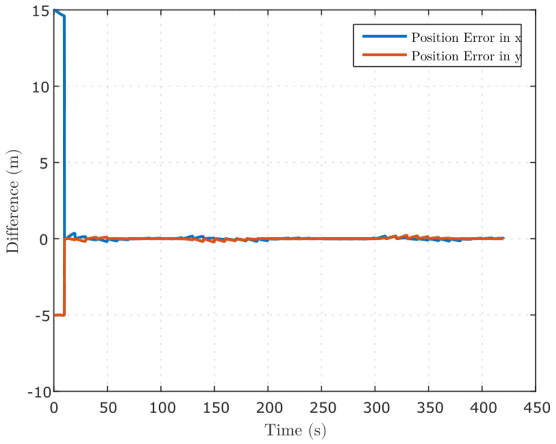

(b) Estimation error in the x and y components

Figure 4: Simulation results for the position estimator.

Finally in figure 5 the complete system is simulated with three vehicles, where two are underwater.

6. Conclusions

The study made on guidance laws stability represents a complete summary of what the literature has to offer in terms of guidance laws for inner loops controlled in yaw. Furthermore, it extends the knowledge on this subject by studying the consequences of applying straight line guidance laws to curved paths, using nonlinear systems stability theory. Practical results are obtained, as for path with constant curvature with the tangent line projection the cross-track error can be controlled to zero and for the along track lookahead distance shows a cross-track error constant and different from zero. For the arbitrary paths the guidance laws are shown to have the same behavior as for the paths with constant curvature.

Secondly, a new method to cancel the effect of currents in the path-following task is designed and tested trough simulation. This new system is separated from the guidance law, definitely decoupling the guidance law from the task to compensate for currents.

Finally, to achieve coordinated motion control of a group of vehicles, a coordination strategy is presented. Moreover, to overcome the stringent communications over acoustic networks, that sometimes will prevent messages to be exchanged among the vehicles, a position estimation is designed for the under water vehicles, and a coordination state estimator is presented for all vehicles to run estimates on the state of its counterparts.

As for future work, it should include tests in the ocean, for this is the only environment that really tests the algorithms developed. In the scope of the algorithms developed, strategies that use range only measurements to compute the underwater vehicle' position can be envisioned, by making the surface vehicle execute pre-defined exciting maneuvers. It

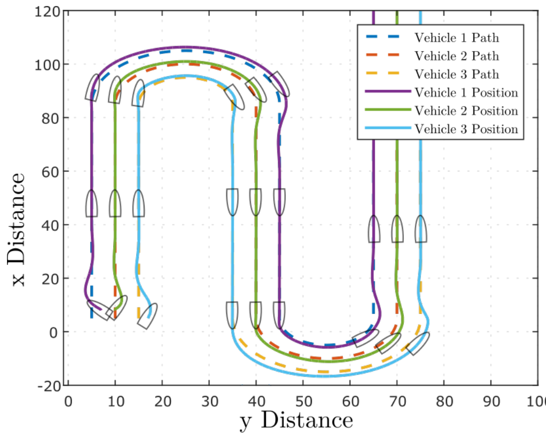

(a) 2D projection

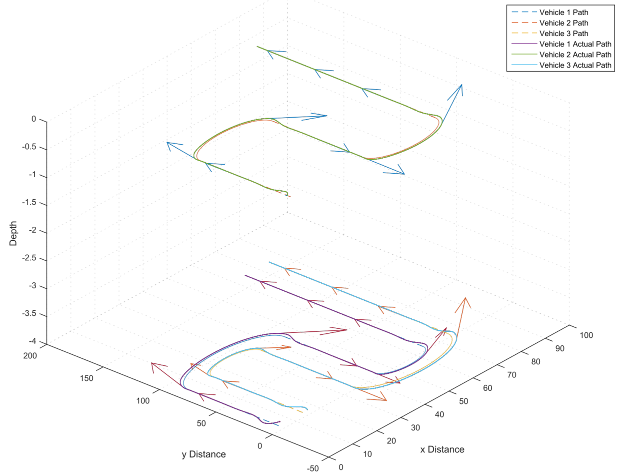

(b) 3D diagram

Figure 5: Cooperative path-following with data exchange occurring with a period of a second.

is an interesting alternative to the use of USBL and can result in a cheaper vehicle's setup.

References

[1] P. C. Abreu. Sensor-based formation control of autonomous underwater vehicles. Master's thesis, IST, Univ. Lisbon, Portugal, December 2014.

[2] G. A. (auth.). *Underwater Robots*. Springer Tracts in Advanced Robotics 96. Springer International Publishing, 3 edition, 2014.

[3] M. Breivik, T. Fossen, et al. Guidance laws for planar motion control. In *Decision and Control, 2008. CDC 2008. 47th IEEE Conference on*, pages 570–577. IEEE, 2008.

[4] J. M. dos Santos Ribeiro. Motion control of single and multiple autonomous marine vehicles. Master's thesis, Instituto Superior Técnico, October 2011.

[5] R. Ghabcheloo, A. Pascoal, C. Silvestre, I. Kaminer, J. A. Hespanha, et al. Coordinated path-following control of multiple underactuated autonomous vehicles in the presence of communication failures. In *Decision and Control, 2006 45th IEEE Conference on*, pages 4345–4350. IEEE, December 2006.

[6] J. P. Hespanha et al. Trajectory-tracking and path-following of underactuated autonomous vehicles with parametric modeling uncertainty. *Automatic Control, IEEE Transactions on*, 52(8):1362–1379, 2007.

[7] L. Lapierre, D. Soetanto, and A. Pascoal. Nonsingular path following control of a unicycle in the presence of parametric modelling uncertainties. *International Journal of Robust and Nonlinear Control*, 16(10):485–503, 2006.

[8] A. M. Lekkas and T. I. Fossen. Line-of-sight guidance for path following of marine vehicles. *Advanced in marine robotics, LAP LAMBERT Academic Publishing*, pages 63–92, 2013.

[9] P. Maurya, A. Agular, and A. M. Pascoal. Marine vehicle path following using inner-outer loop control. In *8th IFAC International Conference on Manoeuvring and Control of Marine Craft 2009, September 16-18, 2009, Guaruja-Brazil. 6 pp.* IFAC International Conference, 2009.

[10] A. Micaelli and C. Samson. Trajectory tracking for unicycle-type and two-steering-wheels mobile robots. 1993.

[11] F. A. Papoulias. Guidance and control laws for vehicle pathkeeping along curved trajectories. *Applied ocean research*, 14(5):291–302, 1992.

[12] A. Pascoal, I. Kaminer, and P. Oliveira. Navigation system design using time-varying complementary filters. *Aerospace and Electronic Systems, IEEE Transactions on*, 36(4):1099–1114, 2000.

[13] C. Samson. Time-varying feedback stabilization of car-like wheeled mobile robots. *The International journal of robotics research*, 12(1):55–64, 1993.

[14] M. F. Silva Ribeiro. Computer-based cooperative motion planning, programming, and control of autonomous robotic. Master's thesis, IST, Univ. Lisbon, Portugal, October 2013.

[15] D. Soetanto, L. Lapierre, and A. Pascoal. Adaptive, non-singular path-following control of dynamic wheeled robots. In *Decision and Control, 2003. Proceedings. 42nd IEEE Conference on*, volume 2, pages 1765–1770. IEEE, 2003.

[16] F. Vanni. Coordinated motion control of multiple autonomous underwater vehicles. Master's thesis, IST, Univ. Lisbon, Portugal, July 2007.

[17] F. Vanni, A. P. Aguiar, and A. Pascoal. Nonlinear motion control of multiple autonomous underwater vehicles. *Proc. of CAMS*, 2007.